Journal of Alloys and Compounds 507 (2010) 356–363

Contents lists available at ScienceDirect

Journal of Alloys and Compounds

journal homepage: www.elsevier.com/locate/jallcom

First-principles calculations of structural, electronic and optical properties of $Cd_xZn_{1-x}S$ alloys

N.A. Noor[a], N. Ikram[a], S. Ali[a], S. Nazir[b], S.M. Alay-e-Abbas[c], A. Shaukat[d,*]

[a] Department of Physics, University of the Punjab, Quaid-e-Azam Campus, 54590 Lahore, Pakistan
[b] Physical Sciences and Engineering Division, KAUST, Thuwal, Saudi Arabia
[c] Department of Physics, GC University, Allama Iqbal Road, Faisalabad 38000, Pakistan
[d] Department of Physics, University of Sargodha, Sargodha 40100, Pakistan

ARTICLE INFO

Article history:
Received 25 May 2010
Received in revised form 21 July 2010
Accepted 27 July 2010
Available online 5 August 2010

Keywords:
Mixed binary semiconductors
First-principles calculations
Electronic and optical properties

ABSTRACT

Structural, electronic and optical properties of ternary alloy system $Cd_xZn_{1-x}S$ have been studied using first-principles approach based on density functional theory. Electronic structure, density of states and energy band gap values for $Cd_xZn_{1-x}S$ are estimated in the range $0 \le x \le 1$ using both the standard local density approximation (LDA) as well as the generalized gradient approximations (GGA) of Wu–Cohen (WC) for the exchange-correlation potential. It is observed that the direct band gap $E_g^{\Gamma-\Gamma}$ of $Cd_xZn_{1-x}S$ decreases nonlinearly with the compositional parameter x, as observed experimentally. It is also found that Cd s and d, S p and Zn d states play a major role in determining the electronic properties of this alloy system. Furthermore, results for complex dielectric constant $\varepsilon(\omega)$, refractive index $n(\omega)$, normal-incidence reflectivity $R(\omega)$, absorption coefficient $\alpha(\omega)$ and optical conductivity $\sigma(\omega)$ are also described in a wide range of the incident photon energy and compared with the existing experimental data.

1. Introduction

Over the last 60 years semiconductor technology of type II–VI and III–V compounds has steadily progressed because of their potential use as phosphors, photoconductors and in fabricating optical detectors, light sources and optoelectronic devices. One of the motives to form alloys of these compounds and investigating their properties is the desire to control the energy band gap, which provides the base for achieving optimal range over which optical detectors and other optoelectronic devices operate [1,2]. Structural, mechanical, electronic and optical properties of a large number of III–V semiconductors and II–VI compounds have been extensively studied both theoretically and experimentally because of their technological importance in modern devices. Especially, with the advent of semiconductor nanodevices, the detailed study of semiconducting materials has become crucial. Furthermore, the wide and direct band gap II–VI semiconductors with the possibility of tailoring lattice parameters and band gap through mixing have recently drawn considerable attention because of their use in solar cells, electroluminescent devices, light emitting and laser diodes [3,4].

ZnS, in both zinc-blende (B3) and wurtzite (B4) phases, is extensively used in electroluminescent devices, blue or ultraviolet light emitting diodes, laser diodes, tunable mid infrared lasers and second harmonic generation devices [5]. To exploit their potential utilization in optical devices, a lot of experimental and theoretical work has been done on cadmium and zinc sulfide semiconductors [6–10]. Whereas $Cd_xZn_{1-x}S$ thin films are used as wide band gap window material in heterojunction photovoltaic solar cells as well as in photoconductive devices, $Cd_xZn_{1-x}S$ nanocrystals have also been synthesized at $x = 0.5$ [11–14]. While efforts to fabricate $Cd_xZn_{1-x}S$ films using starting solutions including both cadmium and zinc nitrates have been undertaken to investigate physical properties of both ZnS and CdS [15], not much of work on the electronic band structure and total energy calculations of the ternary alloys $Cd_xZn_{1-x}S$ has been reported in the literature.

In this paper, we have calculated the structural, electronic and optical properties of binary compounds ZnS, CdS as well as their ternary alloys $Cd_xZn_{1-x}S$, and have compared our results with experiment and other available theoretical studies.

2. Computational details

The calculations for the structural, electronic and optical properties of $Cd_xZn_{1-x}S$ are performed using the full-potential linear-augmented plane wave (FP-LAPW) method within the

* Corresponding author. Tel.: +92 48 9230 618; fax: +92 48 9230 671.
E-mail address: schaukat@gmail.com (A. Shaukat).

0925-8388/$ – see front matter © 2010 Elsevier B.V. All rights reserved.
doi:10.1016/j.jallcom.2010.07.197

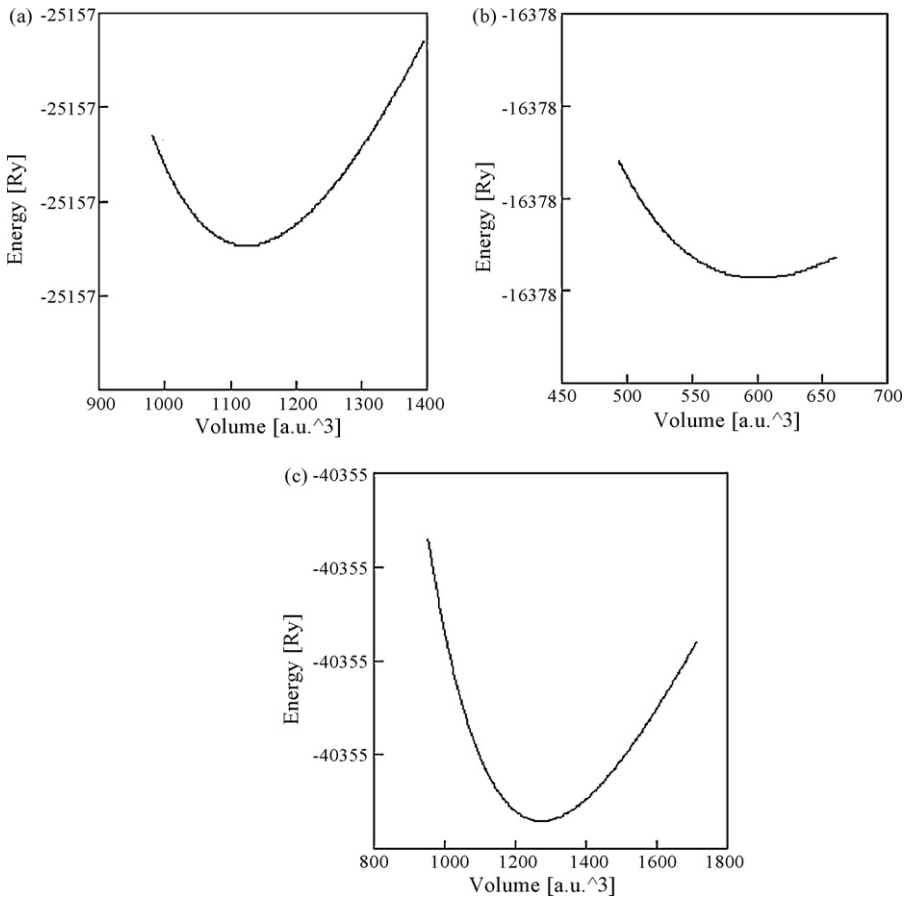

Fig. 1. Variation of total energy as a function of volume for (a) $Cd_{0.25}Zn_{0.75}S$, (b) $Cd_{0.50}Zn_{0.50}S$, and (c) $Cd_{0.75}Zn_{0.25}S$.

framework of the density functional theory (DFT) as implemented in the WIEN2K code [16]. The choice of approximate functional used for determining exchange-correlation energy (E_{xc}) in a Kohn–Sham calculation strongly affects the accuracy of final results. For a crude determination of E_{xc} the exchange-correlation functional in the standard local density approximation (LDA) formalism can be utilized. However, since electron density in solids is inhomogeneous and valence electron density varies relatively slowly with space, a better approach to determine E_{xc} is to utilize generalized gradient approximation (GGA) for calculating electronic and optical properties. In this work, the exchange-correlation potential have been treated using the LDA as well as the GGA. The structural properties are evaluated in both the schemes while electronic and optical properties are calculated only in the generalized gradient approximation (GGA) based on Wu–Cohen schemes.

In the FP-LAPW approach, a muffin-tin (MT) model for the crystal potential is assumed. Non-overlapping spheres are drawn around the ion cores and a region of constant potential is taken in the interstitial region, that is, the region between the spheres. For core electrons full relativistic approximation has been used, whereas for valence electrons scalar relativistic approximation is used, and the spin–orbit (SO) coupling is neglected. The wave function, charge density and potentials are expanded in terms of spherical harmonics within the spheres, and a plane wave expansion is used in the interstitial region. The radius of the MT sphere (R_{MT}) for each atom of the compound is so chosen that there is no charge leakage from the core, and the total energy convergence is ensured. The R_{MT} values for Zn and Cd are taken to be 1.98 a.u., whereas for S the value of R_{MT} is selected to be 1.76 a.u. The maximum value for the angular momentum quantum number $l_{max} = 10$

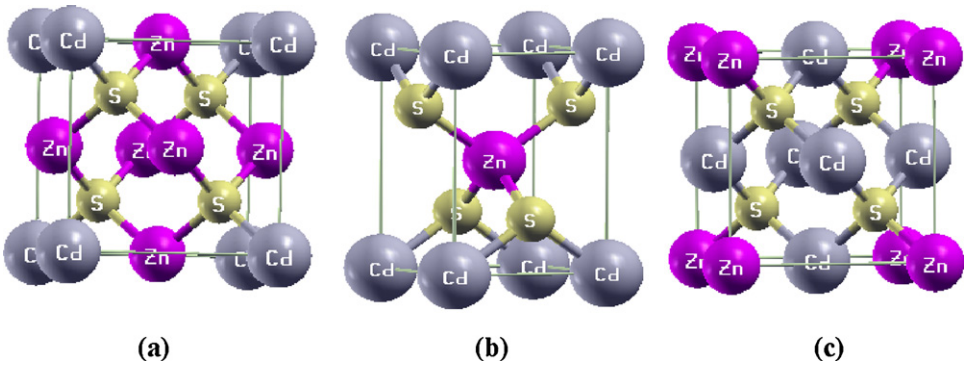

Fig. 2. Crystal Structures of ternary alloys (a) $Cd_{0.25}Zn_{0.75}S$, (b) $Cd_{0.50}Zn_{0.50}S$, and (c) $Cd_{0.75}Zn_{0.25}S$.

is taken for the wave function expansion inside the atomic spheres. In order to get the energy eigenvalue convergence, $K_{max} \times R_{MT} = 7$ is used for the binary compounds ZnS and CdS, whereas for the ternary alloys $Cd_xZn_{1-x}S$, we have used $K_{max} \times R_{MT} = 9$, where K_{max} denotes the maximum value of the reciprocal lattice vector **k**. Both the muffin-tin radius and the number of **k**-points are adjusted to ensure convergence. A mesh of 72 **k**-points for the binary compounds and 35 **k**-points for the ternary alloy were taken for the Brillion zone integrations in the corresponding irreducible wedge. However, a finer **k**-mesh was used in the calculation of dielectric function and related optical properties. The self-consistent calculations process was repeated until the total energy convergence was less than 0.00001 Ryd.

3. Results and discussions

3.1. Structural properties

We have calculated the structural properties of the binary compounds ZnS, CdS and their ternary alloy $Cd_xZn_{1-x}S$ using both the LDA and GGA schemes for the exchange-correlation functional. Volume optimization was performed by minimizing the total energy with respect to the unit cell volume using Murnaghan's equation of state (EOS) [17]. The results of volume optimization for $Cd_xZn_{1-x}S$ at $x = 0.25$, 0.50 and 0.75 are shown in Fig. 1. The crystal structure (of zinc-blende type) for both end compounds ZnS and CdS belongs to space group $F\bar{4}3m$ (no. 216), while for the compositional parameter $x = 0.25$ and 0.75, where Zn is replaced by Cd at the apex and face-center sites, it belongs to the space group $P\bar{4}3m$ (no. 215). Similarly, for the composition $x = 0.50$, the resultant crystal structure belongs to the space group $P\bar{4}m2$ (no. 115), which is a tetragonal structure. The crystal structures of $Cd_xZn_{1-x}S$ for compositional parameter $x = 0.25$, 0.50 and 0.75 have been shown in Fig. 2.

From the volume optimization, equilibrium structure parameters such as the lattice constant '*a*' and the bulk modulus *B* and its pressure derivative *B*′ are estimated, Table 1. It can be readily seen that the calculated values of '*a*' and *B* for the end binaries are in good agreement with the experimental and other theoretical values. The values of the bulk modulus for $Cd_xZn_{1-x}S$ alloys as a function of *x* are also presented in Fig. 3, and it is noticed that its behavior slightly deviates from Vegard's law [18].

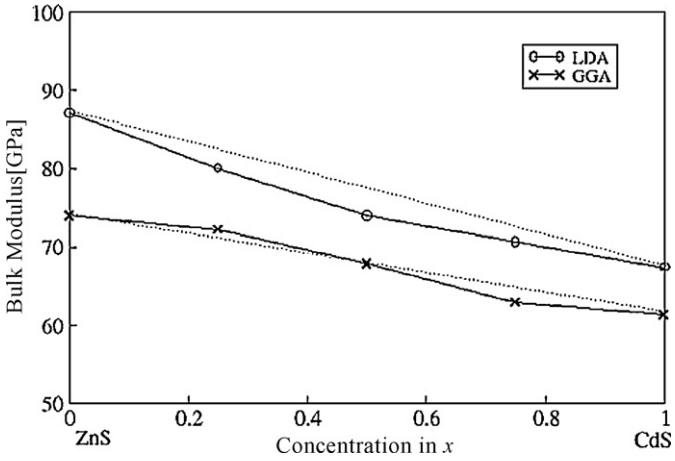

Fig. 3. Composition dependence of calculated bulk modulus using LDA (circles), WC GGA (crosses), and Vegard's law (dotted lines) for $Cd_xZn_{1-x}S$.

3.2. Electronic properties

Analysis of electronic and optical properties of crystalline solids requires the knowledge of electronic density of states (DOS). The DOS for $Cd_xZn_{1-x}S$ at $x = 0.0$, 0.25, 0.50, 0.75 and 1.0 in various phases have been calculated using WC GGA scheme. As we know, Zn, Cd and S have the valence electron configurations $3d^{10}\,4s^2$, $4d^{10}\,5s^2$ and $3s^2\,3p^4$, respectively. Fig. 4 shows the total density of states (TDOS) along with the Cd s and d, Zn d and S s partial density of state (PDOS) for $Cd_xZn_{1-x}S$ for different concentration of *x*. Both ZnS and CdS in B3 phase show a distinct energy gap between the valence and the conduction energy bands, As one can see (Fig. 4), Zn 3d and 4s

Table 1
Calculated lattice parameter '*a*', bulk modulus '*B*' and its pressure derivative '*B*′' for $Cd_xZn_{1-x}S$ at equilibrium volume compared to other theoretical calculations and experiment.

$Cd_xZn_{1-x}S$ $0 \le x \le 1$		LDA	GGA (WC)	Experimental work	Other theoretical work
ZnS	*a* (Å)	5.31	5.36	5.41[a]	5.3998[b], 5.580[c], 5.280[d]
	B (GPa)	87.13	73.97	76.9[a]	80.97[b], 75.9[c], 83.3[d], 83.1[e]
	B′	4.003	4.50		4.73[b]
$Cd_{0.25}Zn_{0.75}S$	*a* (Å)	5.44	5.503		
	B (GPa)	79.98	72.21		
	B′	5.00	4.507		
$Cd_{0.50}Zn_{0.50}S$	*a* (Å)	3.90	3.98		
	c (Å)	5.56	5.62		
	B (GPa)	74.01	67.88		
	B′	4.67	4.37		
$Cd_{0.75}Zn_{0.25}S$	*a* (Å)	5.66	5.74		
	B (GPa)	70.65	62.91		
	B′	4.40	4.27		
CdS	*a* (Å)	5.76	5.83	5.82[f]	5.94[g], 5.81[h], 5.80[i]
	B (GPa)	67.40	61.37	62[f]	55.8[g], 72.42[h], 70.3[i]
	B′	5.038	4.297		4.31[h]

[a] Refs. [32,33].
[b] Ref. [34].
[c] Ref. [35].
[d] Ref. [36].
[e] Ref. [37].
[f] Ref. [38].
[g] Ref. [39].
[h] Ref. [40].
[i] Ref. [41].

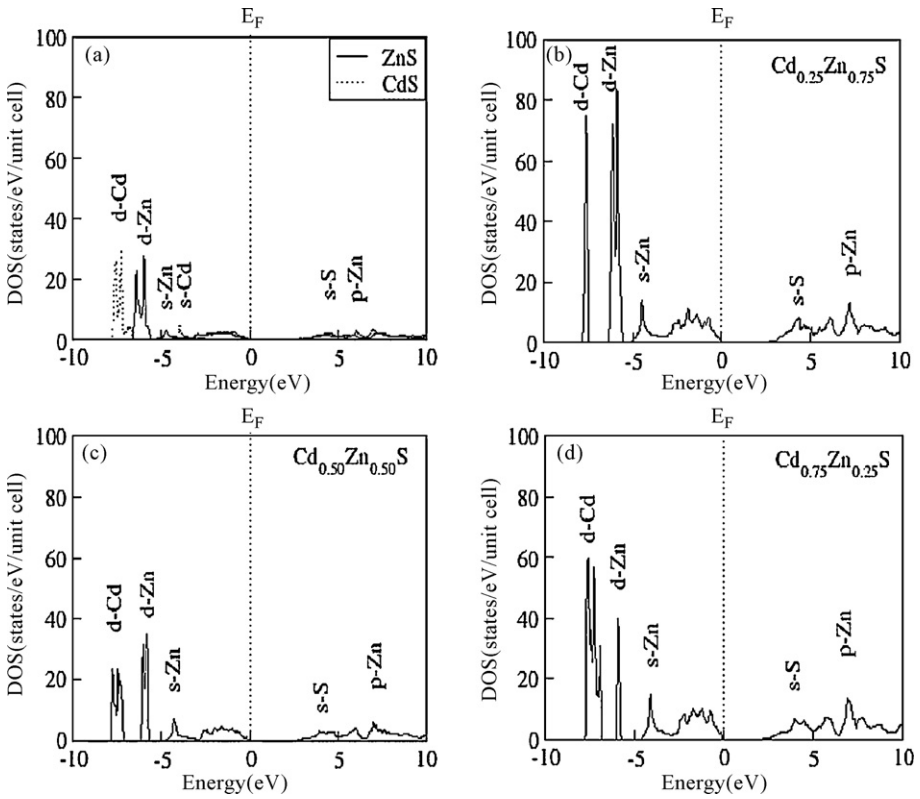

Fig. 4. TDOS (a) ZnS and CdS, (b) $Cd_{0.25}Zn_{0.75}S$, (c) $Cd_{0.50}Zn_{0.50}S$, and (d) $Cd_{0.75}Zn_{0.25}S$.

states in ZnS, and Cd 4d and 5s states form the valence band in CdS, respectively, whereas S 3s state form the conduction band for the two binaries. When the ternary alloy $Cd_xZn_{1-x}S$ ($x = 0.25$, 0.50 and 0.75) is formed, the lower part of the valence band is totally occupied by Cd 4d and Zn 3d states and the upper part of the valence band is occupied by Zn 4s state while the lower part of the conduction band is dominated by S 3s state, the alloy system retaining its semiconducting character.

The band structure calculations give a direct band gap $E_g^{\Gamma-\Gamma}$ for $Cd_xZn_{1-x}S$ for all concentrations of Cd as shown in Table 2. The band gap decreases continuously with the increase of Cd concentration. The evidence of decrease in direct band gap with the increase of composition x has also been observed in experiments on sintered CdZnS films by the screen printing method [19]. Calculated electronic band structures of $Cd_xZn_{1-x}S$ for $x = 0.25$, 0.50 and 0.75 have been shown in Fig. 5 along the high symmetry directions.

Estimated energy band gap values, $E_g^{\Gamma-\Gamma}$, for different compositional parameter x have been shown in Fig. 6 along with the experimental values obtained from absorption as well as from photoconductivity spectra [20]. The similarity between the nonlinear behaviors of the two curves is remarkable, though the calculated values of the band gap are much smaller than the experimental ones (Fig. 6). The large difference in the calculated values of the band gap as compared to the experimental values can be explained by the fact that both LDA and GGA approximations within framework of DFT underestimate the energy gap values in semiconductors, as the self-interaction error and the absence of derivative discontinuity in the exchange-correlation potential can cause an underestimation the energy band gap up to 50% [21,22].

Table 2
Calculated band gaps for $Cd_xZn_{1-x}S$ at Γ-Γ symmetry points.

Composition	$E_g^{\Gamma-\Gamma}$ (eV)	Experimental work	Theoretical work
ZnS	2.0	3.5[a], 3.45[b]	3.4[c], 3.74[d], 3.73[d]
$Cd_{0.25}Zn_{0.75}S$	1.6		
$Cd_{0.50}Zn_{0.50}S$	1.2	2.73[c]	
$Cd_{0.75}Zn_{0.25}S$	1.0		
CdS	0.9	2.44[a], 2.43[c]	1.65[e]

[a] Ref. [13].
[b] Ref. [12].
[c] Ref. [42].
[d] Ref. [43].
[e] Ref. [37].

3.3. Optical properties

Optical properties of $Cd_xZn_{1-x}S$ have been studied experimentally [23–25] but, to the best of our knowledge, no theoretical work based on first-principles calculations has been reported so far. In the present study, we present our theoretical results for some of the optical properties of ternary alloys $Cd_xZn_{1-x}S$. As we know, the refractive index of a material, along with the energy band gap, plays a fundamental role in the use of semiconductors and/or their mixed structures as electronic, optical and optoelectronic devices, as their properties are greatly influenced by the nature and magnitude of these two fundamental physical aspects. Whereas, the band gap determines the absorption threshold of photon in the semiconducting material, refractive index provides a measure of its transparency to the incident radiation. Likewise, the relation between the energy gap and the high frequency refractive index characterizes the electronic band structure of these materials and has been a subject of various investigations [26,27]. The value of refractive index, which is directly related to another elementary property of the material, that is, the dielectric constant, can be determined through empirical and non-empirical approaches, summarized in the above references. Other optical properties, such as absorption coefficient, extinction coefficient, reflectivity, can then be obtained from theses fundamental quantities.

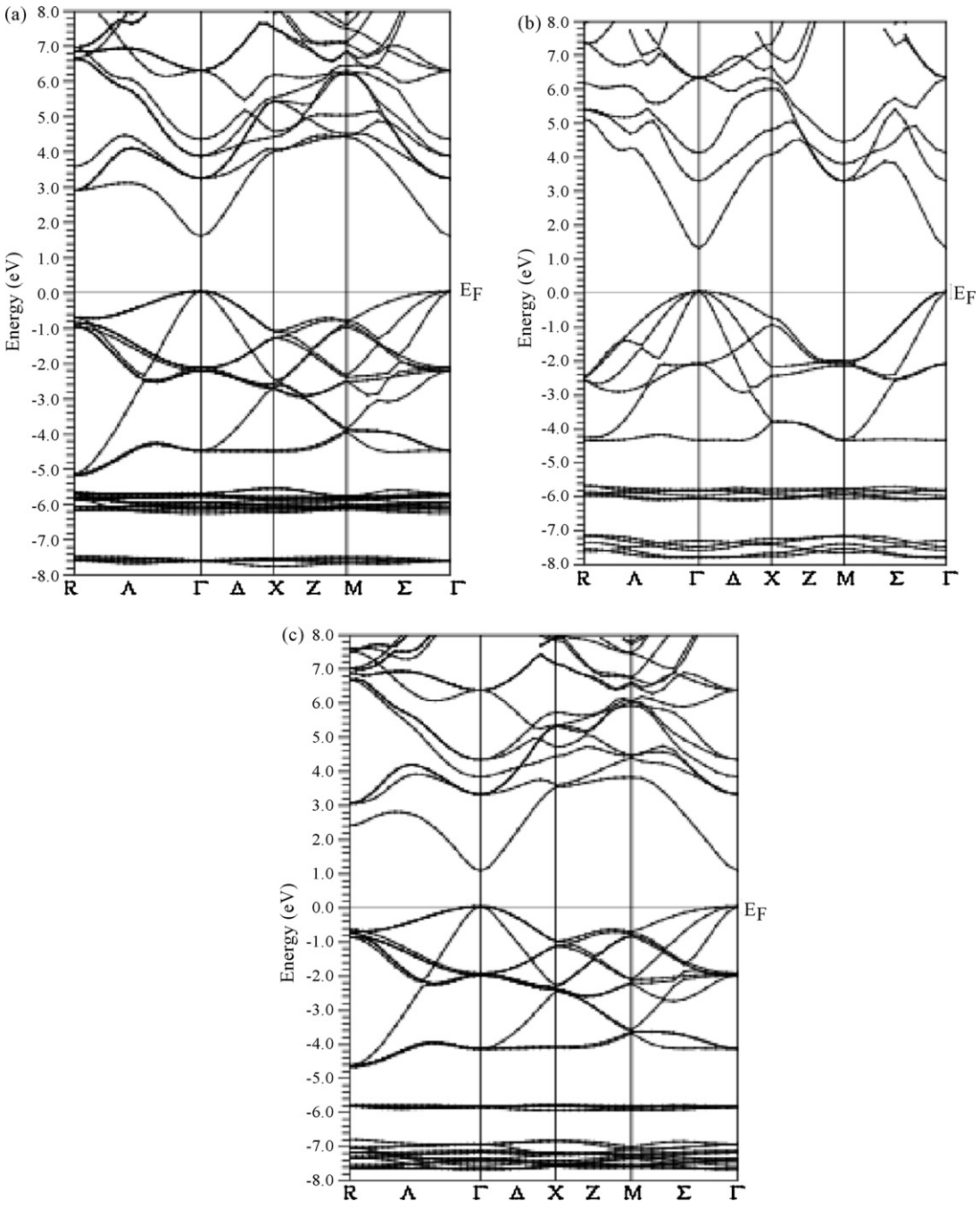

Fig. 5. Band structure for (a) $Cd_{0.25}Zn_{0.75}S$, (b) $Cd_{0.50}Zn_{0.50}S$, and (c) $Cd_{0.75}Zn_{0.25}S$.

In solids various interband and intraband optical transitions are possible that correspond to the electronic band structure of these materials. These transitions can be identified by computing the tensor components of the complex dielectric function $\varepsilon(\omega)$. In case of semiconductors the intraband transitions are not important, whereas the important interband transitions can be further divided into direct and indirect transitions. The indirect interband transitions can be neglected since they are responsible for scattering of phonons and do not contribute to $\varepsilon(\omega)$.

For the alloy system under study, the dielectric function $\varepsilon(\omega) = \varepsilon_1(\omega) + i\varepsilon_2(\omega)$ is calculated as a function of incident photon energy $E = \hbar\omega$ in the range 0–40 eV for the composition $x = 0.0, 0.25, 0.50, 0.75, 1.0$. Next, we evaluate other optical parameters such as complex refractive index and reflectivity. Following Khan et al. [28], the frequency dependent imaginary part of dielectric function for crystals with cubic symmetry can be calculated by:

$$\varepsilon_2(\omega) = \frac{8}{3\pi\omega^2} \sum_{nn'} \int_{BZ} |P_{nn'}(k)|^2 \frac{dS_k}{\nabla\omega_{nn'}(k)}, \tag{1}$$

where the terms on the right hand side have their usual meanings. $\varepsilon_2(\omega)$ is strongly correlated to the joint density of the states (DOS) and momentum matrix element. The real part of dielectric function is obtained from $\varepsilon_2(\omega)$ using the Kramers–Krönig relation [29].

$$\varepsilon_1(\omega) = 1 + \frac{2}{\pi} P \int_0^{\infty} \frac{\omega' \varepsilon_2(\omega')}{\omega'^2 - \omega^2} d\omega' \tag{2}$$

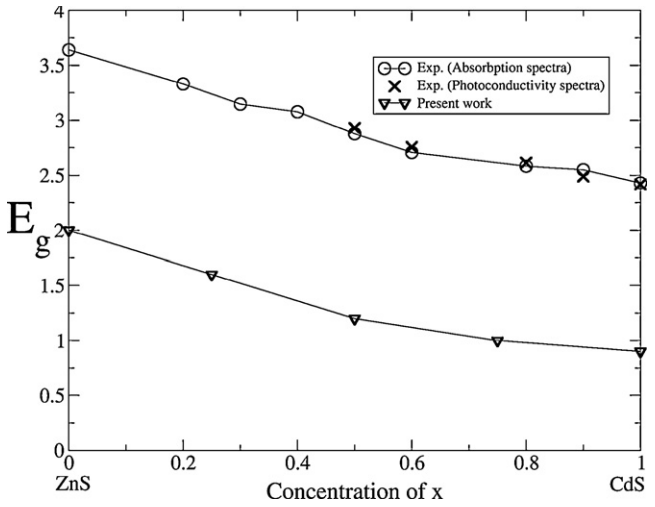

Fig. 6. $E_g^{\Gamma-\Gamma}$ as a function of x, experimental and theoretical curve.

We have carried out our calculations using 3500 **k**-points in the irreducible Brillioun zone. The critical points in Fig. 7(a), occur at about 1.98 eV, 1.51 eV, 1.27 eV, 0.85 eV and 0.67 eV corresponding to $x = 0.0$, 0.25, 0.50, 0.75, 1.0, respectively, and are attributed to the threshold for the direct optical transitions occurring at 2.1 eV, 1.7 eV, 1.36 eV, 1.14 eV and 1.0 eV, respectively. It is observed that the overall behavior of $\varepsilon_2(\omega)$ appears to be similar for all concentrations of Cd with some difference in details.

Table 3
Calculated optical parameters for $Cd_xZn_{1-x}S$ at different Cd concentrations.

x	$E_g^{\Gamma-\Gamma}$ (eV)	$\varepsilon_1(0)$	$R(0)$	$n(0)$	Critical point values			
					ε_2	K	A	σ
0	2.0	6.38	0.19	2.51	1.98	1.86	2.16	2.22
0.25	1.6	6.44	0.20	2.62	1.51	1.56	1.74	1.68
0.5	1.2	6.53	0.21	2.65	1.27	1.21	1.45	1.55
0.75	1.0	6.58	0.22	2.69	0.85	0.97	0.97	1.09
1	0.9	6.61	0.23	2.72	0.67	0.67	0.67	0.91

In Fig. 7(b), we present the real part of the dielectric function, which for ZnS $\varepsilon_1(\omega)$ is positive up to 6.1 eV. It has a small peak at 2.08 eV and passes through double peaks at 4.05 eV and 5.61 eV and again shows a small peak at 7.17 eV, and it becomes negative beyond 7.41 eV. In CdS $\varepsilon_1(\omega) > 0$ up to 7.06 eV, having peaks at 1.09 eV, 3.58 eV, 5.44 eV, and 6.83 eV. For $Cd_{0.75}Zn_{0.25}S$ and $Cd_{0.50}Zn_{0.50}S$, $\varepsilon_1(\omega)$ is positive up to 7.12 eV and 7.22 eV, respectively, whereas in case of $Cd_{0.25}Zn_{0.75}S$ $\varepsilon_1(\omega)$ again shows a small peak around 7.06 eV. It is noted that the binary compounds ZnS

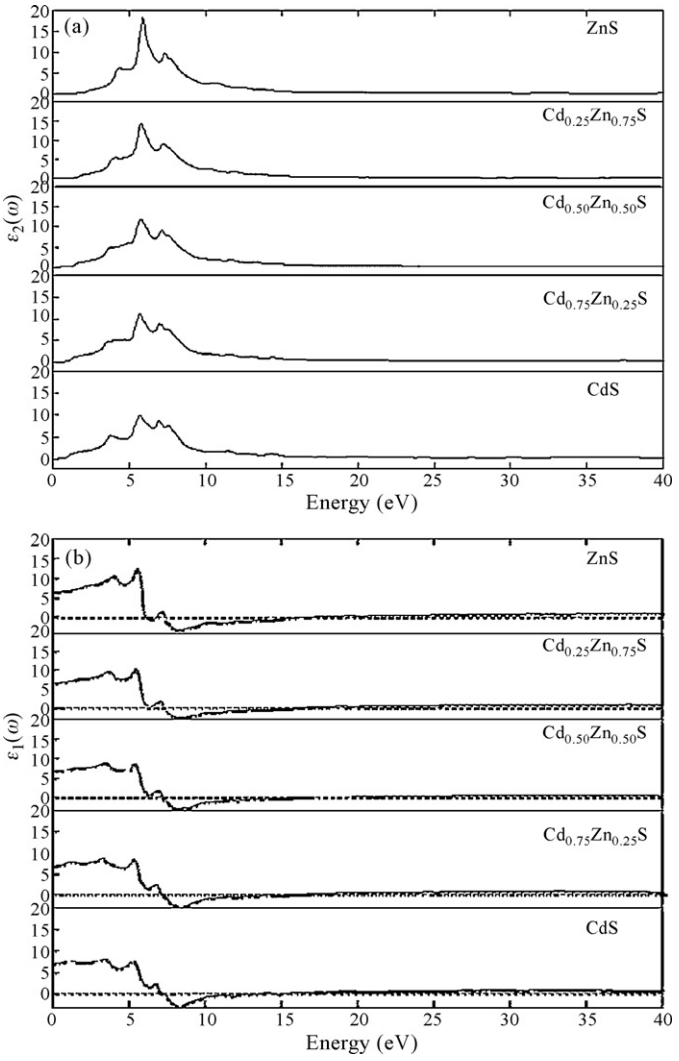

Fig. 7. Dielectric constant for $Cd_xZn_{1-x}S$ corresponding to different values of x, (a) $\varepsilon_2(\omega)$ and (b) $\varepsilon_1(\omega)$.

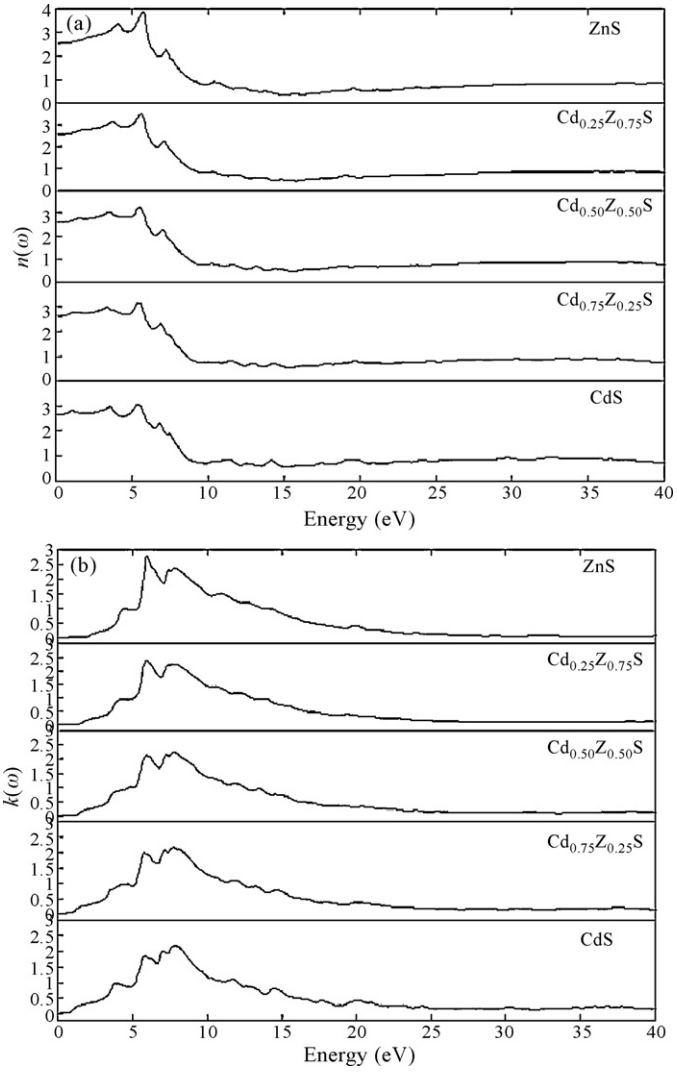

Fig. 8. Complex refractive index for $Cd_xZn_{1-x}S$ corresponding to different values of x, (a) $n(\omega)$ and (b) $k(\omega)$.

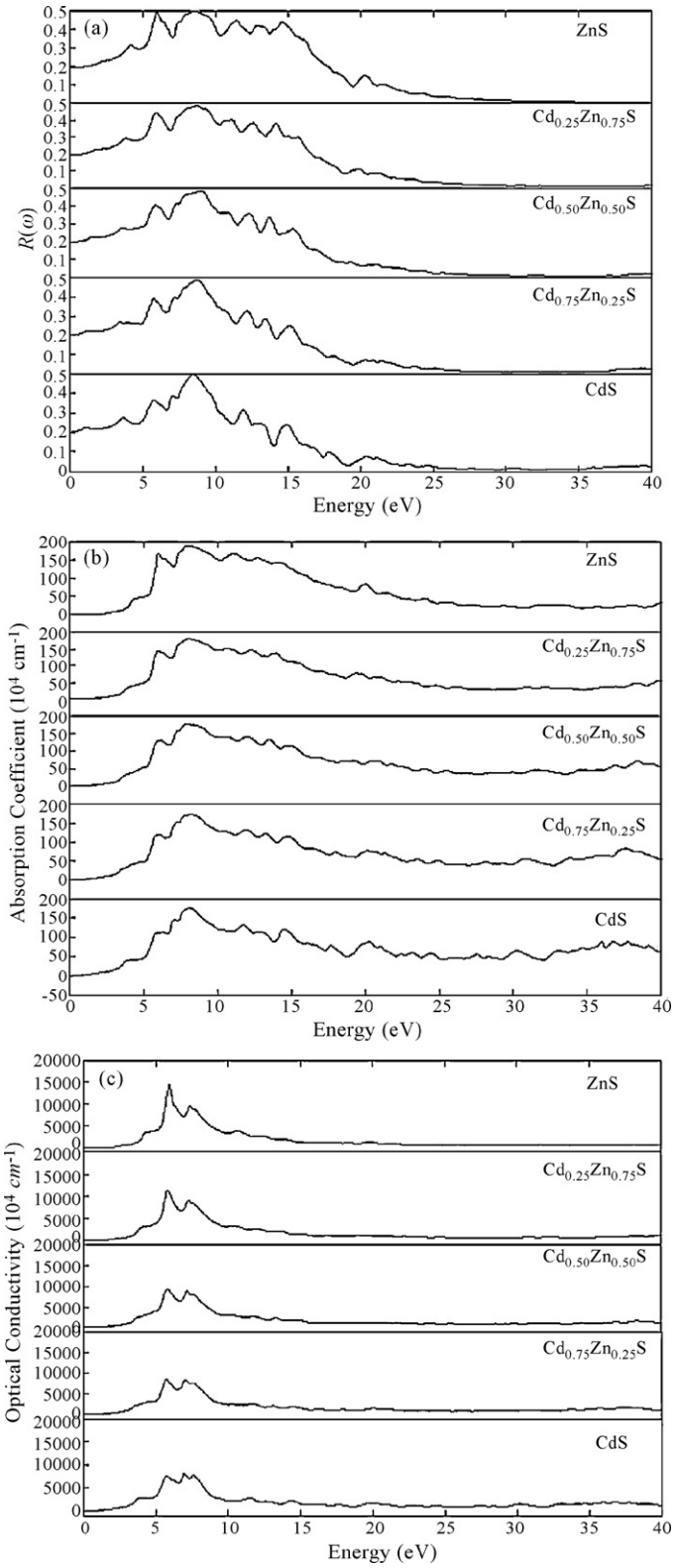

Fig. 9. (a) Reflectivity $R(\omega)$, (b) absorption coefficient $\alpha(\omega)$ and (c) optical conductivity $\sigma(\omega)$ for $Cd_xZn_{1-x}S$ corresponding to different values of x.

and CdS have strong absorption regions in the range 5.14–8.1 and 4.8–7.3 eV, respectively. In these energy ranges, $\varepsilon_1(\omega)$ goes from maximum to minimum and these features are also reflected in the ternary alloys. When $\varepsilon_1(\omega) > 0$, photons propagate through the alloy and for $\varepsilon_1(\omega) < 0$ the electromagnetic wave is damped and for $\varepsilon_1(\omega) = 0$, only longitudinally polarized waves are possible. From recently conducted experimental studies on ZnCdS thin films by Okoli et al. [15], the average value of the real part of the dielectric function is found to be 6.92, which is surprisingly close to our estimated value of the static dielectric function, $\varepsilon_1(0)$, which lies between 6.38 and 6.61.

The critical points of transition for $Cd_xZn_{1-x}S$ are given in Table 3. An important quantity of $\varepsilon_1(\omega)$ is the zero frequency limit $\varepsilon_1(0)$, which represents the dielectric response to the static electric field. In $Cd_xZn_{1-x}S$, $\varepsilon_1(0)$ increases from 6.38 to 6.61 and the direct band gap $E_g^{\Gamma-\Gamma}$ decreases from 2.0 eV to 0.9 eV as x increases from 0 to 1. This shows that the static dielectric constant is inversely proportional to the onset of optical transitions in the alloy. Dependence of the dielectric function on the energy gap can be understood in the context of the Penn model [30]. According to this model, $\varepsilon(0) \approx 1 + (\hbar\omega_p/E_g)^2$, where ω_p is the plasma frequency and E_g is the energy band gap; this relation clearly suggests an increase in the dielectric function with the decrease in the band gap. Similar behavior has also been observed in recent experiments on SiOC films by Yu et al. [31]. Since our calculated values of the band gaps are quite underestimated and, because of the direct relationship between the dielectric constant and the refractive index, our calculated values of the refractive index are a bit overestimated. Our calculated values of the refractive index for ZnS and CdS—the end binary semiconductors are, however, in reasonable agreement with other theoretical results [27]. Similarly, all other optical properties, which have been described in the present study, are influenced to some extent by underestimated values of the band gap, as these properties, as mentioned earlier, are derived from the two fundamental quantities, namely, the refractive index and the band gap. The features of $\varepsilon_1(\omega)$ are closely related to the real part of the complex refractive index, $n(\omega)$, Fig. 8(a). The critical points in $n(\omega)$ vary according to the direct band gap value, $E_g^{\Gamma-\Gamma}$. The value of the calculated refractive index of $Cd_xZn_{1-x}S$ between 3.5 (maximum) and 3.1 (minimum) does not lie very far from the experimental values 2.64 (maximum) and 2.62 (minimum) of ZnCdS thin films, as determined by Okoli et al. [15]. Fig. 8(b) shows the behavior of the extinction coefficient, $k(\omega)$. The reflectivity, $R(\omega)$, depends on both $\varepsilon_1(\omega)$ and $\varepsilon_2(\omega)$, and it is observed that in ZnS, $R(\omega)$ passes through a minimum at 10.23 eV which corresponds to incident photon frequency 1.55×10^{16} rad/s. The next minimum is at 19.37 eV which corresponds to a frequency 2.94×10^{16} rad/s. $R(\omega)$ falls to zero beyond 34.67 eV. As the concentration of Cd in the ternary alloy increases, the reflectivity changes as shown in Fig. 9(a). Furthermore, we have calculated the absorption coefficient $\alpha(\omega)$ and the optical conductivity, $\sigma(\omega)$, which are shown Fig. 9(b) and (c), respectively. A comparative analysis of $\alpha(\omega)$ with electronic band structure presented in Fig. 5 reveals the manner in which incident radiation may get absorbed in these materials. The S atom s states and Zn and Cd atom s like states play a major role in these optical transitions as initial and final states for these alloys. The threshold of the optical conductivity of the ternary alloys $Cd_xZn_{1-x}S$ at 2.5 eV, as calculated in the present study, seems to lie close to the 2.0 eV value of the experimental study on ZnCdS thin films [15], the energy range in the optical conductivity plot in the two studies may differ appreciably.

4. Conclusions

We have calculated the structural, electronic properties and optical properties of $Cd_xZn_{1-x}S$, using FP-LAPW approach in the framework of the DFT, The density of states calculations indicate that the Zn 3d and Cd 4d states dominate the lower part and Zn 4s state the upper part of the valence band, while the S 3s state prevails in the lower part of the conduction band. The variation

of the direct energy band gap $E_g^{\Gamma-\Gamma}$ in $Cd_xZn_{1-x}S$, as estimated from the calculated electronic band structure, agrees well qualitatively with experimental results, Furthermore, the calculations for the dielectric constant $\varepsilon(\omega)$ show that smaller energy gap $E_g^{\Gamma-\Gamma}$ yields a larger static dielectric constant $\varepsilon_1(0)$ and refractive index varies as $\varepsilon_1(0)$. For all values of x in $\varepsilon_2(\omega)$ curves, the critical points correspond to direct optical transitions. Reasonable agreement can be found between some of the optical properties calculated in this work and the experimental results from a recently conducted study on ZnCdS thin films. The overall features of real and imaginary parts of the complex dielectric functions are similar for $Cd_xZn_{1-x}S$ alloys over all compositions ranges (x = 0.0, 0.25, 0.50, 0.75 and 1.0). However the major maxima in the spectra of $\varepsilon_2(\omega)$ and $\varepsilon_1(\omega)$ seem to decrease as one goes from ZnS to CdS. Furthermore, the calculated reflectivity spectra for the ternary alloys $Cd_xZn_{1-x}S$ show that there are regions of maximum and minimum reflectivity, which shift with x, and this feature may be utilized in the fabrication of optoelectronic devices.

References

[1] M.C. Gupta, J. J. Ballato (Eds.), Handbook of Photonics, Taylor & Francis, 2006.
[2] H.E. Ruda, Wide-gap II–VI Compounds for Opto-electronic Applications, Springer, 1992.
[3] K.T.R. Reddy, P.J. Reddy, J. Phys. D 25 (1992) 1345.
[4] F. Benkabou, H. Aourag, M. Certier, Mater. Chem. Phys. 66 (2000) 10.
[5] Z.J. Xin, R. Peaty, H.N. Rutt, R.W. Eason, Semicond. Sci. Technol. 14 (1999) 695.
[6] C.G. Van der Walle, Phys. B 185 (1993) 1.
[7] T.A. Chnoweth, R.H. Bube, J. Appl. Phys. 51 (1980) 1844.
[8] A.D. Corsa, S. Baroni, R. Resta, S. Gironcoli, Phys. Rev. B 47 (1993) 3588.
[9] T. Okamoto, Y. Matsuzaki, N. Amin, A. Yamada, M. Konagai, Jpn. J. Appl. Phys. 37 (1998) 3894.
[10] D. Hariskos, M. Ruck, T. Walter, H.W. Schock, Proc. 1st WCPEC, Hawaii, 1994, p. 91.
[11] E. Dutková, P. Baláž, P. Pourghahramani, A.V. Nguyen, V. Šepelák, A. Feldhoff, J. Kováč, A. Šatka, Solid State Ionics 179 (2008) 1242.
[12] S. Arora, S.S. Manoharan, Opt. Mater. 31 (2008) 176.
[13] P. Kumar, A. Misra, D. Kumar, N. Dhama, T.P. Sharma, P.N. Dixit, Opt. Mater. 27 (2004) 261.
[14] J. Torres, G. Gordillo, Thin Solid Films 207 (1992) 231.
[15] (a) M.K. Karanjai, D.D. Gupta, Thin Solid Films 155 (1987) 309;
(b) D.N. Okoli, A.J. Ekpunobi, C.E. Okeke, Acad. Open Internet J. 18 (2006) 1.
[16] P. Blaha, K. Schwarz, G.H. Madsen, D. Kvasnicka, J. Luitz, FP-L/APW+lo Program for Calculating Crystal Properties, K. Schwarz, Techn. WIEN2K, Austria, 2001.
[17] F.D. Murnagham, Proc. Natl. Acad. Sci. 30 (1944) 244.
[18] L. Vegard, Z. Phys. 5 (1921) 17.
[19] V. Kumar, V. Singh, S.K. Sharma, T.P. Sharma, Opt. Mater. 11 (1998) 29.
[20] V.P. Singh, S. Singh, Czech. J. Phys. B 26 (1976) 1161.
[21] R.W. Godby, M. Schlüter, L.J. Sham, Phys. Rev. Lett. 56 (1986) 2415.
[22] M. Städle, J.A. Majevski, P. Vogel, A. Görling, Phys. Rev. Lett. 79 (1997) 2089.
[23] J. Torres, J.I. Cisneros, G. Gordillo, F. Alvarez, Thin Solid Film 289 (1996) 238.
[24] S.C. Ray, M.K. Karanjai, D.D. Gupta, Thin Solid Films 322 (1998) 117.
[25] A.H. Ammar, Phys. B 296 (2001) 312.
[26] N.M. Ravindra, P. Ganapathy, J. Choi, Infrared Phys. Technol. 50 (2007) 21.
[27] M.A. Salem, Chin. J. Phys. 42 (2003) 288.
[28] M.A. Khan, A. Kashyap, A.K. Solanki, T. Nautiyal, S. Auluck, Phys. Rev. B 23 (1993) 16974.
[29] F. Wooten, Optical Properties of Solids, Academic, New York, 1972.
[30] D.R. Penn, Phys. Rev. 128 (1962) 2093.
[31] Y.H. Yu, S.C. Lee, C.S. Yang, C.K. Choi, W.K. Jung, J. Korean Phys. Soc. 42 (2003) 682.
[32] O. Madelung, M. Schultz, H. Weiss, Physics of II–IV and I–VII Compounds. Semimagnetic Semiconductors, Landolt Börnstein New Series group III, vol. 17, Pt. b, Springer, Berlin, 1982.
[33] K.H. Hellwege, O. Madelung (Eds.), Semiconductors, Intrinsic properties of group IV elements and III–V, II–VI and I–VII Compounds, Landolt-Börnstein New Series group III, vol. 22, Pt. a, Springer, Berlin, 1982.
[34] R. Gangadharan, V. Jayalakshmi, J. Kalaiselvi, R. Murugan, B. Palanivel, J. Alloys Compd. 359 (2003) 22.
[35] J.E. Jaffe, R. Pandey, M.J. Seal, Phys. Rev. B 47 (1993) 6299.
[36] A. Nazzal, A. Qteish, Phys. Rev. B 53 (1996) 8262.
[37] A. Qteish, M. Parrinello, Phys. Rev. B 61 (2000) 6521.
[38] O. Madelung, M. Schulz, H. Weiss, Numerical Data and Functional Relationships in Science and Technology, Landolt-Borstein, vol. 17, Springer, Berlin, 1982.
[39] S. Zerroug, F. Ali Sahraoui, N. Bouarissa, Eur. Phys. J. B 57 (2007) 9.
[40] E. Deligoz, K. Colakoglu, Y. Ciftci, Phys. B 373 (2006) 124.
[41] S. Wei, S.B. Zhang, Phys. Rev. B 62 (2000) 6944.
[42] N. Fitzer, A. Kuligk, R. Redmer, Phys. Rev. B 67 (2003) 201201.
[43] S. Nazir, N. Ikram, S.A. Siddiqi, Y. Saeed, A. Shaukat, A.H. Reshak, Curr. Opin. Solid State Mater. Sci. 14 (2010) 1.